Design and Analysis of Stationary Frame PR Current Controller for Performance Improvement of Grid Tied PV Inverters

A.Chatterjee
Department of Electrical Engineering
National Institute of Technology
Rourkela, India
contactaditi247@gmail.com

K.B. Mohanty
Department of Electrical Engineering
National Institute of Technology
Rourkela, India
kbmohanty@nitrkl.ac.in

***Abstract*— In this paper a single phase grid connected photovoltaic (PV) system has been modeled and simulated using Matlab/Simulink. The PV generator is interfaced with the utility grid by a single phase voltage source inverter (VSI). A maximum power point tracking (MPPT) control algorithm is implemented to extract maximum power from the PV generator irrespective of operating conditions. The DC-DC boost converter placed in between PV generator and VSI performs MPPT and amplifies the output voltage from PV array to desired level. A control strategy to regulate the quality of power injected by the grid connected VSI is proposed. Two controllers are designed for the grid side DC-AC inverter one is the proportional integral (PI) voltage controller which regulates the DC link voltage, the other is the Proportional + Resonant (PR) current controller which maintains the current injected by the inverter into grid in phase with the grid voltage so that unity power factor can be achieved. A harmonic compensator (HC) is cascaded with PR controller to mitigate low order odd harmonic components present in the output current of VSI and minimize the total harmonic distortion (THD). Simulation results validate the effectiveness of the proposed control strategy.**

Keywords*— *DC-DC converter, Harmonic compensator Maximum power point tracking, Proportional Integral controller, Proportional Resonant controller, Total harmonic distortion.

I. INTRODUCTION

Diminution of fossil fuel reserves and increased concern about environmental pollution has amplified the demand of renewable energy sources (RES) for power generation. Moreover to meet the escalating electricity demand more distributed generation (DG) plants based on wind and solar energy are integrated into power distribution system. The form in which power is generated by the DG plants may not be compatible with the conventional distribution system such as DC output from fuel cells, photovoltaic modules and batteries, variable frequency AC output from wind turbines etc. To alter the generated power into the required format power electronics converters are required. Single phase distribution system is often used to serve the rural and residential areas and the PV plants are mostly installed in these areas. To interface the PV units with the grid single phase inverters are required.

Different converter topologies have been proposed for single phase grid connection of PV modules [1]. One is the single stage topology where the PV module is connected to the grid through a single DC-AC inverter. In that case the inverter performs MPPT to extract out the maximum power from the module and also voltage amplification to step up the output voltage to desired value. The other one is the dual stage topology where there is a DC-DC converter after the PV unit. In this case DC-DC converter handles the task of maximum power extraction and also boosts the voltage as per requirement. In this paper two power processing stage topology has been implemented. The grid side DC-AC converter which injects power into the grid has to ensure that the quality of power is good. The basic tasks which the grid side converter handles includes control of active and reactive power exchange between the grid and PV system and synchronization of grid current with grid voltage.

Various control strategies have been proposed to enhance current control of the grid tied VSIs. [2]. Basically these controllers are categorized into three major classes: 1)synchronous frame controller 2)stationary-frame controller 3)natural-frame controller. In synchronous or d-q frame control the control variables are transformed from natural frame to a synchronous rotating frame (frame rotates synchronously with grid voltage). Hence the control variables appear as dc quantities and the control is better. The PI controllers are associated with this control structure. The major drawback associated with this structure is the necessity to extract the phase angle of grid voltage and incorporating the voltage feed forward and cross coupling terms in the control loop. In stationary or α-β frame control structure the control variables are time varying. The Proportional Resonant (PR) controllers falls under the category of stationary frame controllers are simple to design and has excellent reference signal tracking capabilities. The PR controllers can achieve very high gain at resonant frequency thus reducing the steady state error to zero [3-5]. More over harmonic compensators can be used to mitigate low order harmonic without influencing behavior of the current controller. Hence they are superior than PI controllers in terms of eliminating steady state errors and harmonic current rejection. The natural or abc

frame control structure is usually implemented for non linear controllers such as hysteresis and dead beat control. The drawback associated with these controllers is variable switching frequency.

II. SINGLE PHASE GRID TIED PHOTOVOLTAIC SYSTEM

Based on the number of power processing stages the possible inverter topologies are given below [1]: (i) Single stage (ii) Dual stage

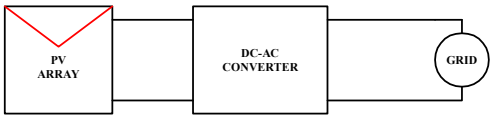

Fig.1 (a) Single stage grid tied PV array

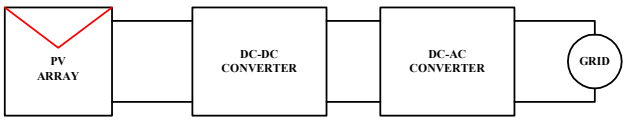

Fig.1 (b) Dual stage grid tied PV array

In single power processing stage as shown in Fig.1(a) the DC-AC converter is responsible for voltage amplification, MPPT and grid current control and in dual power processing stage shown in Fig.1(b) the DC-DC converter handles MPPT, voltage amplification and the DC-AC converter handles the grid current control. The former topology is used for past centralized PV inverter technology. In this case the inverter has to be designed to handle peak power of twice the nominal power of the system. The later topology is mostly used in present day multi-string technology. Here the PV inverter is designed to handle only the nominal system power. In this research work the dual stage topology is implemented.

A. Dual Power Processing Structure for Single Phase Grid Tied PV System

Figure.2. shows the schematic diagram of a single phase grid tied PV system where the PV generator is interfaced with the grid via two converters [2]. Two controllers are designed.

a)Input side controller: a MPPT controller is designed to estimate the output voltage and current from the PV array and extract maximum power from the source. It generates reference voltage for the front end DC-DC converter.

b)Grid side controller: the task of the grid side controller is to control power flow between the DG source and grid, ensure good quality of power injected by the inverter into the grid and grid synchronization.

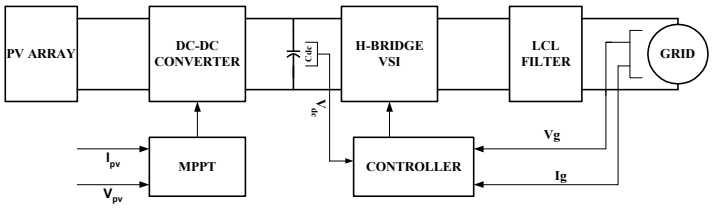

Fig. 2. Schematic diagram of grid tied photovoltaic system

B. Modeling of PV Array

The selection of PV array depends on the power rating of the system. Solar cell is basically a p-n junction fabricated on a layer of semiconductor, when sun rays strikes the surface of cell, the solar energy gets converted to electrical energy. The output of a single PV cell usually vary between 0.8 volts to 1.2 volts which is not suitable for practical applications. The output of a single cell can be scaled up as desired to meet the system power requisite. Cells are connected in series to raise the voltage level and in parallel to increase the current level. Individual PV cells allied in series and parallel form a PV module and appropriate association of modules make a PV array. The solar panel used in this paper is KC200GT and the parameters of the panel at 25^{0}C, AM 1.5, and irradiance 1000 W/m^2 is tabulate in Table I. 10 number of such panels are connected in series to obtain a power output of 2000 Watts. Fig.3 and Fig.4 demonstrate the PV curve and IV curve obtained by simulating the PV array model in MATLAB [6].

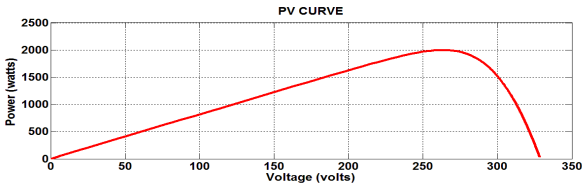

Fig. 3. PV curve at STC

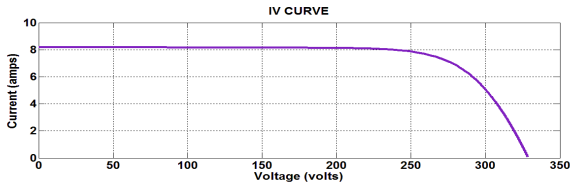

Fig.4. IV curve at STC

TABLE I. Parameters of KC200GT ,PV array at STC

Parameters	Values
Maximum Power, P_{max} (W)	200.143
Current at P_{max}, I_{mp} (A)	7.61
Voltage at P_{max}, V_{mp} (V)	26.3
Short circuit current I_{sc} (A)	8.21
Open circuit voltage V_{oc} (V)	32.9
Number of cells in series	54

C. Maximum Power Point Tracking

There is a unique point on the PV curve where the photovoltaic panel delivers maximum power which is known as the maximum power point (MPP). The power output of the PV panel may vary with the atmospheric conditions like temperature, irradiance etc. So in order to draw maximum power from the solar array a MPP tracking algorithm is

integrated with the PV system. Various MPPT algorithms have been reported in literature [7], among which the incremental conductance (IC) algorithm is applied in this work. This algorithm is based on the observation that at MPP, the condition that occurs is given by (1a):

$$\frac{dp}{dv} = 0 \tag{1a}$$

$$\frac{dp}{dv} = I + v\frac{dI}{dv} \tag{1b}$$

$$I + v\frac{dI}{dv} > 0 \tag{1c}$$

$$I + v\frac{dI}{dv} < 0 \tag{1d}$$

When (1b) is satisfied the operating point is at MPP. When the condition given by (1c) and (1d) is met the operating point is at left and right of MPP respectively. From (1c) and (1d) it can be determined in which direction perturbation must occur to budge the operating point towards the MPP and the perturbation is repeated until (1a) is satisfied. Once the MPP is reached, the algorithm continues to operate at this point until an alteration in current is detected.

The MPPT controller estimates the output voltage and current of the PV array and generates the reference voltage for the front end DC-DC boost converter. The front end converter maintains a constant DC link voltage irrespective of the input voltage level from the PV array. The value of the boost inductor can be calculated from (2) and the DC link capacitance can be calculated from (3) [8].

$$L_b = \frac{D(1-D)^2 T_s V_0}{2 * I_0} \tag{2}$$

$$C_{dc} = \frac{P_{dc}}{2 * \omega * V_{dc} * \Delta V_{dc}} \tag{3}$$

Where D is duty ratio, T_s is switching time and V_0 and I_0 are the output voltage and current respectively. ω is grid frequency P_{dc} and V_{dc} are the DC link power and voltage respectively. ΔV_{dc} is amplitude of voltage ripple which varies between 1% to 5%.

III. CONTROLLER DESIGN FOR SINGLE PHASE GRID TIED VSI

Two controllers are developed for the single phase grid tied inverter: The inner current controller and the outer voltage controller. The current controller takes care of the quality of current injected into the grid and the power exchange between the system and grid. The voltage controller regulates the DC link voltage and generates reference current signal for current loop. The VSI is connected to grid via an LCL filter whose parameters are designed from [9] as shown in Fig. 5.The task of the passive filter is to reduce the output current distortion.

A. Orthogonal Signal Generation

To design controller for single phase inverter a signal orthogonal to the original singe phase signal has to be created. Researchers have proposed various orthogonal signal generation methods. Among all, the all pass filter (APF) method [10] is selected for this study because it is not complex and does not attenuate the input signal. The transfer function of the APF is given by (4).

$$\frac{V_{g\beta}}{V_{g\alpha}} = \frac{\omega_f - s}{\omega_f + s} \tag{4}$$

The output of the APF, $V_{g\beta}$ is the voltage signal perpendicular to the original grid voltage and the input $V_{g\alpha}$ is voltage signal aligned with grid voltage, ω_f is the fundamental frequency. The measured grid voltage signal V_g is the input to the filter.

B. DC Link Voltage Controller

The reference dc link voltage is compared with measured voltage of the DC link capacitor and the error is fed to a PI controller, which controls the DC link voltage and generates reference current signal for the inner current control loop as shown in Fig.5. The voltage controller is of the form given by (5).

$$G_v = K_p + \frac{K_i}{s} \tag{5}$$

Where K_p and K_i are the proportional and integral gain of the controller.

C. Synchronized Reference Current Generation

The single phase grid voltage signal is split into two signals orthogonal to each other by APF method as mentioned earlier. By considering the output of the voltage control loop which is the reference current $I_{g\alpha}^{ref}$, parallel to the original voltage signal and the current reference $I_{g\beta}^{ref}$, perpendicular to the grid voltage which is a user input command a reference current synchronized with the grid voltage can be calculated by (6).

$$I_g^{ref} = \frac{I_{g\alpha}^{ref} V_{g\alpha} + I_{g\beta}^{ref} V_{g\beta}}{V_{gmag}} \tag{6}$$

Where V_{gmag} is the magnitude of the grid voltage and given by (7).

$$V_{gmag} = \sqrt{V_{g\alpha}^2 + V_{g\beta}^2} \tag{7}$$

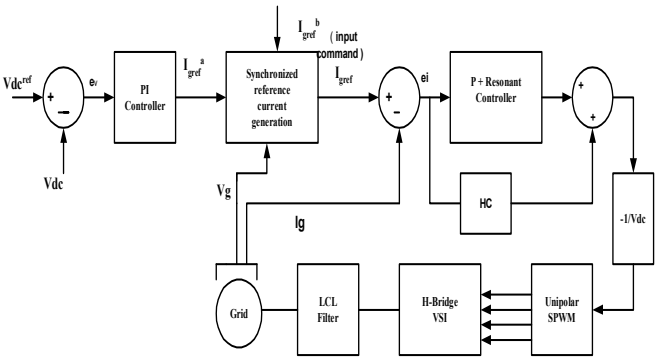

Fig.5. Block diagram for closed loop DC link voltage and grid current control

$I_{g\alpha}^{ref}$ which is in phase with the grid voltage controls the real power of the system and the orthogonal component $I_{g\beta}^{ref}$ controls the reactive power exchange of the system with the grid. Hence a decoupled control of real and reactive power can be achieved [11-12].

D. Proportional Resonant Current Controller

The input to the PR controller is the current error which is obtained by comparing the reference current and the grid current and the output is the voltage signal which is passed to the PWM modulator as shown in Fig.5. Unipolar pulse width modulation technique is implemented to control the switching of the IGBT switches of the single phase VSI. The transfer function of an ideal PR compensator is given by (8) [4-5].

$$G_{pr}(s) = K_p + \frac{2K_i s}{s^2 + \omega^2} \tag{8}$$

Where k_p and k_i are the controller gains and ω is the grid frequency. From frequency response analysis of an ideal PR compensator in Fig.6(a) it was observed that the gain is infinitely high at resonant frequency (grid frequency) and much low at other frequencies. Hence a high gain low pass filter is introduced to reduce the gain and broaden the bandwidth of the controller. The transfer function of non-ideal PR controller is mentioned by (9). From the bode diagram in Fig.6(b) it can be observed that the gain of the controller is much reduced at resonant frequency.

$$G_{npr}(s) = K_p + \frac{2K_i \omega_c s}{s^2 + 2\omega_c s + \omega^2} \tag{9}$$

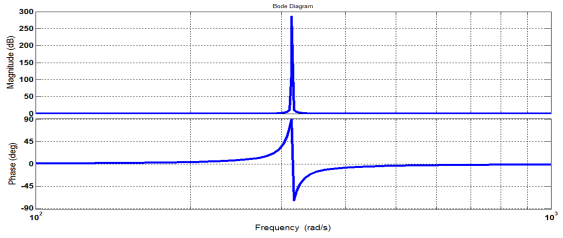

Fig. 6(a) Bode plot for ideal PR compensator

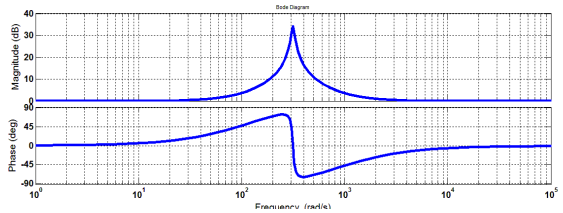

Fig.6(b) Bode plot for non-ideal PR compensator

The parameters of the PR controller are adjusted by performing frequency response analysis. A harmonic compensator is cascaded with the controller to mitigate the odd harmonics of 3rd, 5th and 7th order and to reduce the THD of grid current below 5% as per IEEE 1547 standard for interconnecting distributed generation. The transfer function of the HC is given by (10).

$$G_{hc}(s) = \sum_{n=3,5,7} \frac{2K_{in}s}{s^2 + (n\omega)^2} \tag{10}$$

Where n is the order of harmonics.

E. Stability Analysis of PR Current Controller

The block diagram of current control loop is shown in Fig. 7. The output of the current loop is given by (11) [5].

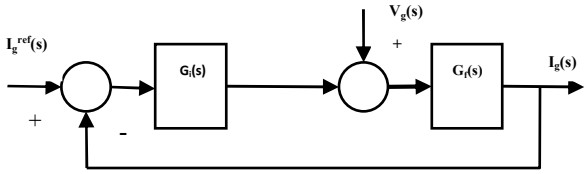

Fig.7. Block diagram of current controller

$$I_g(s) = H_i(s) I_g^{ref}(s) + H_v V_g(s) \tag{11}$$

$$H_i(s) = \frac{G_i(s)G_f(s)}{G_i(s)G_f(s) + 1} \tag{12}$$

$$H_v(s) = \frac{G_f(s)}{1 + G_i(s)G_f(s)} \tag{13}$$

Where $G_i(s)$ and $G_f(s)$ are the transfer functions of the current controller and LCL filter respectively. Where the former is given by (9) and the later is given by (14).

$$G_f = \frac{C_f R_d s + 1}{s^3 L_i L_g C_f + s^2 C_f R_d (L_i + L_g) + s(L_i + L_g)} \tag{14}$$

Where the values of L_g, L_i and C_f are given in Table II.

To obtain zero steady state error and track the reference current signal I_g^{ref} effectively the PR controller introduces very high gain hence $G_i(j\omega)$ value is infinite for ideal PR controller at fundamental frequency. The magnitude of $H_i(j\omega)$ and $H_v(j\omega)$ approaches unity and zero at the same frequency. So, the grid voltage feed forward in the current loop can be detached. The transfer function of the current controller can be given by (15).

$$I_g(s) = H_i(s) I_g^{ref}(s) \tag{15}$$

The closed loop gain of the current control loop with the PR controller is given by (16).

$$G(s) = G_i(s) G_f(s) \tag{16}$$

Where $G_i(s)$ and $G_f(s)$ are given by (9) and (14) respectively. Fig.8(a) and Fig.8(b) shows the bode plot of the current loop gain with the PR compensator and with the harmonic compensator respectively.

From the frequency response plot it can be observed that the phase margin and gain margin have large positive value, which demonstrate the closed loop stability of the system. On adding the harmonic compensator the only change that can be

observed is appearance of gain peaks at harmonic frequencies but the dynamics of the controller, in terms of bandwidth and stability margin remains unaltered.

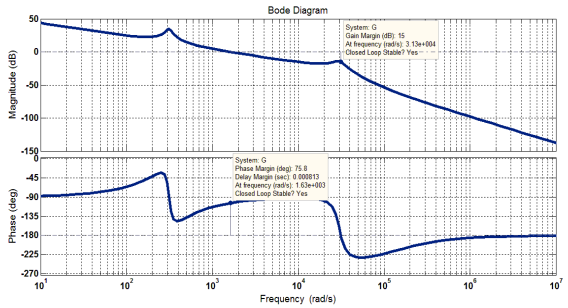

Fig. 8(a). Bode plot of compensated current loop gain

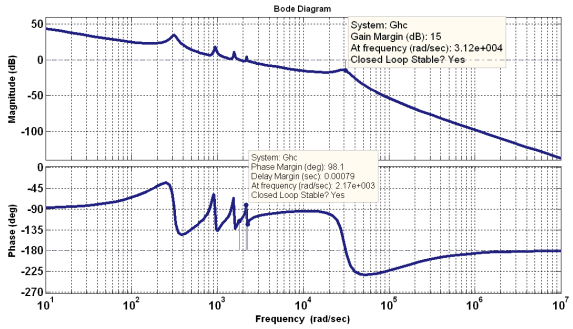

Fig. 8(b). Bode plot of compensated current controller loop gain with HC

TABLE II. Simulation parameters

Grid voltage (V_g)	230 V (rms)
DC link voltage (V_{dc})	400 V
DC link capacitor (C_{dc})	2 mF
Inverter side inductance (L_i)	12.5 mF
Grid side inductance (L_g)	0.312 mF
Filter capacitance (C_f)	3.612 µF
Filter damping resistance (R_d)	2.38 Ohms
Boost inductor (L_b)	0.5 mH
Switching frequency (f_{sw})	10 Hz

IV. SIMULATION RESULTS AND DISCUSSION

Simulation study is performed on a 2 kW single phase grid tied PV system. The simulation parameters are tabulated in Table II. The simulation results confirm the efficacy of the proposed control strategy.

A. Steady State Operation

The reactive current command is set to zero and the system is simulated for 0.5 sec the objective is to extract 2 kW of power from the PV system and inject it to grid. Fig. 9(a) gives the grid voltage waveform and current waveform superimposed on it. From which it can be observed that the voltage and current are in same phase. Fig. 9(b) shows the power waveforms which reveal that the system only delivers a constant active power and the reactive power is almost zero.

From FFT analysis waveform given in Fig.9(c) it can be observed that the THD of the grid current is 2.66% which is much below the prerequisite standard.

B. Dynamic Operation

To study the dynamic response of the system the reference reactive current command is changed from +6.14 A to -6.14 A at 0.45 s. Fig. 10(a) shows the grid voltage waveform with current waveform superimposed on it. From the figure it can be observed that when reactive power command is changed, the current starts lagging the voltage waveform. Hence the operating power factor also changes. The power waveforms given in Fig. 10(b) reveal that when there is a step change in reactive power command at 0.45 s the reactive power output changes from +1000 W to -1000 W at 0.45 s but the real power output remains constant. This demonstrates the decouple control of power.

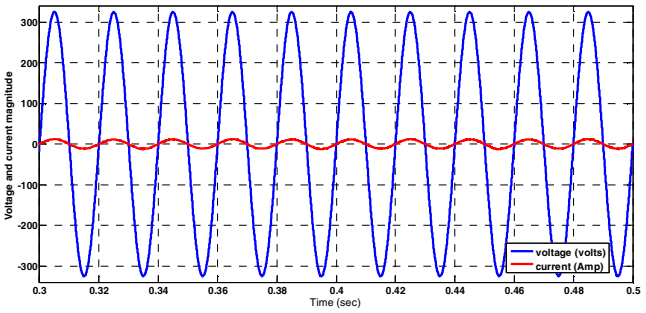

Fig.9(a). Grid voltage and current waveform

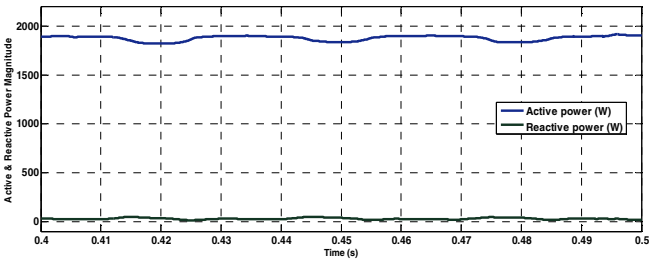

Fig. 9(b). Real and reactive power waveforms.

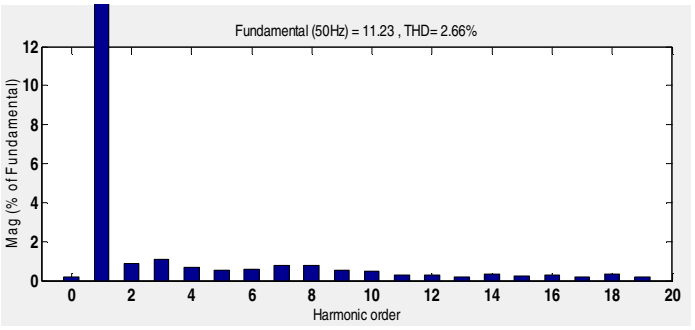

Fig. 9(c). FFT analysis waveform of grid current

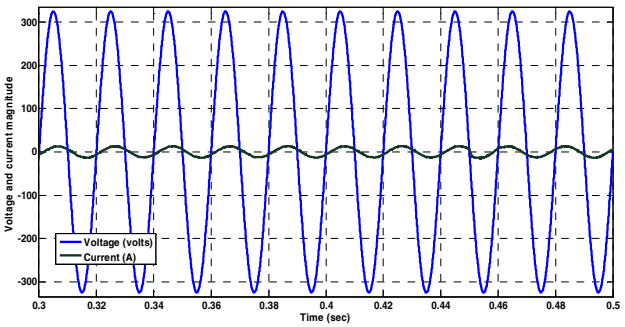

Fig. 10(a). Grid current waveform

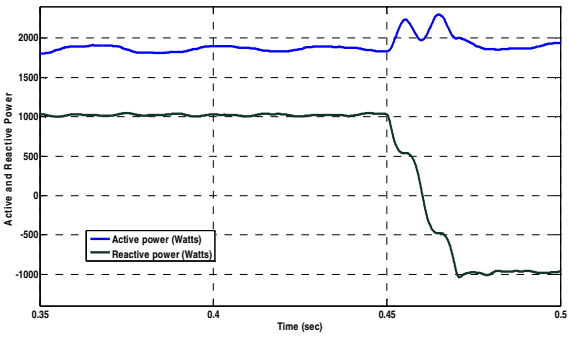

Fig. 10(b). Real and reactive power waveforms

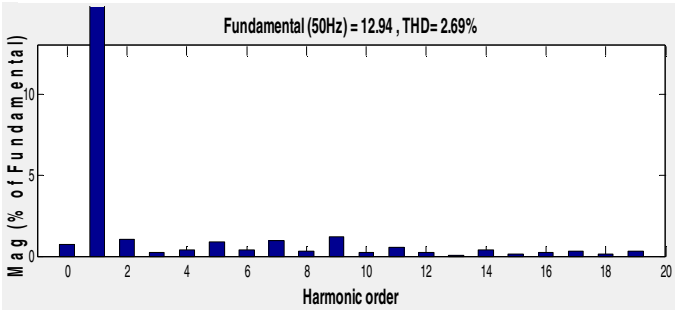

Fig. 10(c). FFT analysis waveform of grid current

Fig. 10(c) shows the FFT analysis waveform of the grid current during dynamic operation. From the waveform it can be observed that the THD is 2.69% which is below 5%.

V. CONCLUSION

This paper has proposed a stationary frame PR controller to regulate the power exchange between the PV inverter and grid. The current injected by inverter into the grid is aligned with the grid voltage. A harmonic compensator cascaded with the PR current controller reduces the THD of grid current. Stability analysis of the current controller is performed which reveals that the current controller is stable.

REFERENCES

[1] S. B. Kjaer, J. K. Pedersen, and F. Blaabjerg, “A review of single-phase grid-connected inverters for photovoltaic modules,” IEEE Trans. Ind. Appl., vol. 41, no. 5, pp. 1292–1306, Sep./Oct. 2005.

[2] F. Blaabjerg, R. Teodorescu, M. Liserre, and A. V. Timbus, “Overview of control and grid synchronization for distributed power generation systems,” IEEE Trans. Ind. Electron., vol. 53, no. 5, pp. 1398–1409, Oct. 2006.

[3] D. N. Zmood and D. G. Holmes, “Stationary frame current regulation of PWM inverters with zero steady-state error,” IEEE Trans. Power Electron., vol. 18, no. 3, pp. 814–822, May 2003.

[4] M. Castilla, J. Miret, J. Matas,” Linear Current Control Scheme With Series Resonant Harmonic Compensator for Single-Phase Grid-Connected Photovoltaic Inverters” IEEE Trans. on Ind. Electronics, vol. 55, no. 7, pp. 2724-2733, July 2008.

[5] H. Cha, T.-K. Vu, and l.-E. Kim, "Design and control of proportional resonant controller based photovoltaic power conditioning system," in Energy Conversion Congress and Exposition, ECCE, IEEE, pp. 2198 - 2205, Sept. 2009.

[6] Marcelo Gradella Villalva, Jonas Rafael Gazoli, and Ernesto Ruppert Filho, “Comprehensive Approach to Modeling and Simulation of Photovoltaic Arrays,” IEEE Trans. Power Electron., Vol. 24, no. 5, pp.1198-1208, May 2009.

[7] Mohamed A. Eltawil, Zhengming Zhao, ”MPPT techniques for Photovoltaic applications”, Renewable and Sustainable Energy Reviews, Volume 25, Pages 793-813, September 2013.

[8] N. Mohan, T. M. Undeland, and W. P. Robbins, Power Electronics - Converters, Applications, and Design, 2nd ed: John Wiley & Sons, Inc.,1995.

[9] Hyosung Kim, Kyoung-Hwan Kim, “Filter design for grid connected PV inverters”, IEEE International Conference on Sustainable Energy Technologies (ICSET2008), pp.1070-1075, 2008.

[10] R. Y. Kim, S. Y. Choi, and I. Y. Suh, “Instantaneous control of average power for grid tie inverter using single phase DQ rotating frame with all pass filter,” in Proc. IEEE Annu. Conf. Ind. Electron. Soc., pp. 274–279, Nov 2004.

[11] B. Bahrani, A. Rufer, S. Kenzelmann, and L. A. C. Lopes, “Vector Control of Single-Phase Voltage-Source Converters Based on Fictive-Axis Emulation”, IEEE Trans. on Ind. Electronics, vol. 47, no. 2, pp. 831-840, March/April 2011.

[12] S.Samerchur, S.Premrudeepreechacharm, Y.Kumsuwun, K.Higuchi, “Power control of single phase Voltage control Inverter for Grid Connected Photovoltaic Systems", IEEE Proceeding, 978-1-61284- 788-7/11, 2011.